ISSN 0915-633X

NATIONAL INSTITUTE FOR FUSION SCIENCE

Suppression of Plasma Turbulence by Asymmetric Superthermal Ions

K. Itoh, T. Ohkawa, S. -I.Itoh, M. Yagi and A. Fukuyama

(Received - May 22, 1997)

NIFS-496 July 1997

RESEARCH REPORT
NIFS Series

NAGOYA, JAPAN

Suppression of Plasma Turbulence by Asymmetric Superthermal Ions

K. Itoh[1], T. Ohkawa [1,2], S.-I. Itoh[3], M. Yagi[3], A. Fukuyama[4]

[1] *National Institute for Fusion Science, Nagoya 464-01 Japan*

[2] *Department of Physics, University of California San Diego, La Jolla CA, U. S. A.*

[3] *Research Institute for Applied Mechanics, Kyushu University, Kasuga 816 Japan*

[4] *Faculty of Engineering, Okayama University, Okayama 700, Japan*

Abstract

Influence of inhomogeneity of plasma flow on the magnetic surface, which is driven by the anisotropic superthermal ions, on the turbulence of the low/negative magnetic shear tokamak is investigated. It is found that the poloidal asymmetry of the pressure gradient of superthermal ions can suppress the current-diffusive ballooning mode turbulence which causes strong turbulent transport. The critical asymmetry of superthermal ions for the reduction of transport is derived. This theory provides the new mechanism of improved confinement associated with the reversed magnetic shear.

Keywords: improved confinement, reduced magnetic shear, superthermal ions, current-diffusive ballooning mode, turbulent transport

One of the main subjects of the plasma physics is the understanding of the structural formation and turbulent transport of toroidal plasmas. The research has been strongly motivated by the finding of the H-mode[1] and other improved confinement modes. After the theory of the electric field bifurcation for the H-mode has been presented,[2] the roles of the radial electric field structure are investigated widely.[3-5] (See the recent review.[6]) In addition to the role of the radial electric field, the influence of the current profile for the confinement improvement has been studied.[7,8] Very recently, it has been clearly demonstrated that the new type of the improved confinement, which occurs in tokamaks with the reduced/negative magnetic shear, has been confirmed experimentally.[9,10] Although the previous theory based on the radial electric field shear and reduced magnetic shear could provide some understanding of this new improved confinement (see a recent review[11]), an essential understanding is missing. First, there are varieties in such "enhanced reversed shear" ("ERS") mode: The steep gradient of the electron temperature in JT-60U[12] has not been observed in the "ERS" modes of other tokamaks. Furthermore, the directionality of the neutral beam injection, which is considered effective from the model of the electric field shear, is not necessarily crucial in inducing the "ERS"-mode. These facts require understanding of the new mechanism that drives the prominent transport barrier for electrons.

In this article we present a new mechanism of the suppression of the turbulence in the tokamaks with low/negative magnetic shear. We investigate the role of the toroidal plasma flow which is *inhomogeneous on the magnetic surface*. Such an inhomogeneity is sustained by the energetic ions which are inhomogeneous in the poloidal direction.[13] Energetic ions, which are sustained by plasma heating, are usually anisotropic and can be localized either in the low field side or in the high field side. The nonlinear current-diffusive ballooning mode turbulence, which has been known to give understandings of the L-mode and high-β_p-mode[14] as well as the H-mode,[15] is investigated in this article. It is shown that the thermal conductivity of electrons and ions is substantially reduced by the asymmetry of the pressure gradient of superthermal ions. The necessary level of the poloidal-asymmetry of superthermal ions is derived. This new theory gives understanding of the internal electron transport barrier like the one in JT-60U.

A high aspect-ratio and cylindrical tokamak is employed and the quasi toroidal coordinates (r, θ, ζ) are used. The reduced set of equations[16] with electrostatic approximation is employed. The stability and turbulence nature of the ballooning mode are characterized by the magnetic shear $s = rq'/q$ and the normalized pressure gradient $\alpha = -q^2 R\beta'$, where q is the safety factor, R is the major radius of the torus, and β is the ratio of the plasma pressure p_0 to the magnetic pressure $B_0^2/2\mu_0$. When the superthermal ions are anisotropic, the perpendicular pressure, $p_{s,\perp}$, could be dependent on the poloidal angle. We take into account of the poloidally-asymmetric superthermal ions, the pressure gradient of which is characterized as

$$\frac{\partial}{\partial\psi}p_s(\psi, \theta) = \Gamma\,(1 + \cos\theta)\frac{\partial}{\partial\psi}p_0(\psi) \qquad (1)$$

In Eq.(1), ψ is the label of the magnetic surface (the minor radius here) and Γ is the parameter that indicates the magnitude. Combining the force balance equation of the electron fluid (Ohm's law)

$$\vec{E} + \vec{v} \times \vec{B} = \frac{1}{en}\left(-\nabla p_e + \vec{j} \times \vec{B}\right) \qquad (2)$$

with the force balance equation $\vec{j} \times \vec{B} = \nabla p_0 + \nabla p_s$, the rotation velocity is obtained. When the energy of superthermal ions is much higher than that of bulk plasma particles, the poloidal inhomogeneity of the density is small and is neglected here. (That is, the static potential is approximated to be constant on the magnetic surface.) It is also assumed that the plasma is rotating in the toroidal direction, because the central plasma is of interest and the neoclassical damping of poloidal rotation is considered to be strong. Under this circumstance, the toroidal rotation frequency, $\Omega = V_\zeta / R$, is obtained[13] as $\Omega = \Omega_0(r) + \Omega_1(r, \theta)$ with

$$\Omega_1(\theta) = \Gamma\,(1 - \cos\theta)\,\frac{1}{e\bar{n}}\frac{dp_0}{d\psi} \simeq \left(\frac{\Gamma}{2}\,\frac{1}{e\bar{n}}\frac{dp_0}{d\psi}\right)\theta^2 + \cdots \tag{3}$$

where we defined Ω_0 as $\Omega_0 = \Omega(\theta = 0)$. ($\bar{n}$:average density.) The toroidal angular velocity is not constant on the magnetic surface but has the poloidal inhomogeneity.

In the presence of this asymmetric toroidal flow, the nonlinear stability and the associated transport of the current-diffusive ballooning mode are analyzed. By use of the method of the dressed test mode, the nonlinear turbulence is reformulated as an eigenvalue equation in which turbulence is renormalized as turbulent transport coefficients (μ, λ, χ), which are ion viscosity, current diffusivity and thermal diffusivity, respectively.[14,15] The mode with the toroidal mode number n is subject to the Doppler shift of $n\Omega$. Contrary to previous theories, not the radial inhomogeneity of $n\Omega$, but the poloidal inhomogeneity is studied. In the frame which is rotating with the angular frequency at $\theta = 0$, the Doppler shift, $\Delta\Omega$, is given by $\Delta\Omega = n\Omega_1(\theta)$. By replacing the form of Doppler shift in the ballooning equation for the dressed test mode,[15] we have

$$\frac{d}{d\eta}\frac{F}{\hat{\gamma} + \Lambda F^2}\frac{d}{d\eta}\left[\hat{\gamma} + i\Delta\Omega + XF\right]\tilde{p} + \alpha(1 + \Gamma\cos\eta)\left(\kappa + \cos\eta + G\sin\eta\right)\tilde{p}$$
$$-\left[\hat{\gamma} + i\Delta\Omega + MF\right]F\left[\hat{\gamma} + i\Delta\Omega + XF\right]\tilde{p} = 0 \tag{4}$$

where $\hat{\gamma}$ is the growth rate, $\Lambda = \hat{\lambda}n^4q^4$, $K = \hat{\chi}n^2q^2$ and $M = \hat{\mu}n^2q^2$ represent nonlinear interactions, and the relations $\hat{\mu} \simeq \hat{\chi}$ and $\hat{\lambda}/\hat{\chi} \simeq (\delta/a)^2$ hold. (In Eq.(4) and the following, the length and the time are normalized to the minor radius a and poloidal Alfven time τ_{Ap}, respectively, as was in [15]. The symbol hat represents the normalization.) The metric factors $F = 1 + G^2$ and $G = s\eta - \alpha\sin\eta - (\alpha\Gamma/8)\sin 2\eta$ are modified by the poloidal asymmetry of pressure gradient, and the pressure gradient term also includes the Γ-correction as $\alpha(1 + \Gamma\cos\eta)$.[17] Perpendicular mode number is given as $\hat{k}_\perp^2 = Fn^2q^2$. The Doppler shift terms is normalized and expressed as $\Delta\Omega = \hat{\Omega}\,\theta^2/2$ with

$$\hat{\Omega} = nq\,\Gamma\left(-p_0'/e\tilde{n}B_p v_A\right).$$

In the absence of the asymmetric superthermal ions, the nonlinear eigenvalue equation (4) was solved, and the turbulent transport coefficients have been derived.[15] As in [15], Eq.(4) is approximated by the Weber-type equation assuming that the mode is localized near $\eta < 1$. In order to obtain the analytic insight, the limit of small α and s are analyzed. In this case, the relation $\alpha\Lambda/X \simeq 1$ was found[15] and the corrections $\hat{\gamma}/\Lambda$ and $\hat{\Omega}/\Lambda$ are higher order terms in comparison with $\hat{\gamma}/X$ and $\hat{\Omega}/X$. Keeping the effects of the poloidally-inhomogeneous rotation, Eq.(4) is approximated as

$$\left[\frac{d^2}{d\eta^2} + \frac{\Lambda}{X}\alpha\left\{1 - \frac{MX}{\alpha} + \Gamma + \left(\frac{\alpha + X^2}{\alpha X}\right)i\hat{\omega}\right\} - \frac{\Lambda}{X}\alpha\left(1 + 2\Gamma + \left(\frac{\alpha + X^2}{\alpha X}\right)i\hat{\Omega}\right)\frac{\eta^2}{2}\right]\tilde{p}(\eta) = 0 \tag{5}$$

$(\hat{\gamma} \rightarrow -i\hat{\omega})$. This eigenmode equation is solved, and the nonlinear eigenvalue equation is given as

$$\frac{\Lambda}{X}\alpha - M\Lambda + \frac{\Lambda}{X}\alpha\left(\Gamma + \left(\frac{\alpha + X^2}{\alpha X}\right)i\hat{\omega}\right) = \sqrt{\frac{1}{2}\frac{\Lambda}{X}\alpha\left(1 + 2\Gamma + \left(\frac{\alpha + X^2}{\alpha X}\right)i\hat{\Omega}\right)} \tag{6}$$

with the eigenfunction

$$p(\eta) = exp\left(-\frac{\sigma}{2}\eta^2\right) \tag{7}$$

and $\sigma = \Lambda X^{-1}\alpha - M\Lambda + \Lambda X^{-1}\alpha(\Gamma + i\hat{\omega}(\alpha + X^2)/\alpha X)$. Equation (6) is expanded with respect to Γ and $\hat{\omega}$ as

$$\begin{aligned}\frac{\Lambda}{X}\alpha - \sqrt{\frac{1}{2}\frac{\Lambda}{X}\alpha} - M\Lambda \simeq \left(-\frac{\Lambda}{X}\alpha + \sqrt{\frac{1}{2}\frac{\Lambda}{X}\alpha}\right)\Gamma \\ + i\left(\frac{\alpha + X^2}{\alpha X}\right)\left(-\frac{\Lambda}{X}\alpha\hat{\omega} + \sqrt{\frac{1}{2}\frac{\Lambda}{X}\alpha}\,\frac{\hat{\Omega}}{2}\right) + \sqrt{\frac{1}{2}\frac{\Lambda}{X}\alpha}\left(\frac{\alpha + X^2}{\alpha X}\right)^2\frac{\hat{\Omega}^2}{8}\end{aligned} \tag{8}$$

In the limit of Γ, $\alpha \rightarrow 0$, solutions have been given as[14,15]

$$\hat{\chi} = \hat{\chi}_L(s, \alpha \to 0) \simeq \frac{1}{\sqrt{2}} \frac{\hat{\lambda}}{\hat{\chi}} \sqrt{\frac{\hat{\chi}}{\hat{\mu}}}\ \alpha^{3/2} \tag{9a}$$

with

$$\alpha\Lambda/X - \sqrt{\alpha\Lambda/2X} - M\Lambda \simeq 0\ , \tag{9b}$$

$n^2q^2 = \hat{k}_\theta^2 = (\hat{\chi} / \hat{\lambda})\, \alpha^{-1}$, and $\alpha\Lambda/X \simeq 1$. Coefficients of the terms in the right hand side of Eq.(8) is evaluated by use of the unperturbed solution, Eq.(9). Imaginary part of Eq.(8) gives

$$\hat{\omega} = \frac{1}{2\sqrt{2}}\, \hat{\Omega}\ . \tag{10}$$

The real part of Eq.(8) yields the transport coefficient. For a convenience, we rewrite the coefficient of the $\hat{\Omega}^2$ term in Eq.(8) as $(8\sqrt{2})^{-1}\sqrt{\Lambda\alpha/X}(1/X + X/\alpha)^2 \equiv C_1 M\Lambda\, \alpha^{-1}$ by introducing a coefficient C_1, which is of the order of unity. With this simplification, Eq.(8) is simplified as

$$\frac{\Lambda}{X}\alpha - \sqrt{\frac{1}{2}\frac{\Lambda}{X}\alpha} - M\Lambda = M\Lambda\left(-\Gamma + \frac{C_1}{\alpha}\,\hat{\Omega}^2\right) \tag{11}$$

If we compare this eigenvalue equation with the unperturbed one, Eq.(9b), the perturbed equation is obtained from Eq.(9b) by the replacement as $\mu \to (1 - \Gamma + C_1\alpha^{-1}\,\hat{\Omega}^2)\mu$. With this transformation, the transport coefficient, in the presence of asymmetric superthermal ions, is given as

$$\hat{\chi} = \left(\sqrt{1 - \Gamma + C_1\alpha^{-1}\,\hat{\Omega}^2}\right)^{-1} \hat{\chi}_L \simeq \left(1 - \Gamma/2 + C_1\,\hat{\Omega}^2/2\alpha\right)^{-1} \hat{\chi}_L \tag{12}$$

The inhomogeneous rotation frequency and the asymmetric pressure gradient are related. In the expression of $\hat{\Omega}$, $\hat{\Omega} = nq\,\Gamma\left(-p_0'/e\tilde{n}B_p v_A\right)$, the coefficient $\left(-p_0'/e\tilde{n}B_p v_A\right)$

is rewritten as $\alpha(2q)^{-1}\delta a^{-1} m_i^{1/2} m_e^{-1/2}$. By the help of the estimation $nq = \hat{\chi}^{1/2}\hat{\lambda}^{-1/2}\,\alpha^{-1/2} \simeq a\delta^{-1}\alpha^{-1/2}$, we have the relation

$$\hat{\Omega} = \alpha^{1/2}(2q)^{-1} m_i^{1/2} m_e^{-1/2}\,\Gamma.$$

By use of this relation, the suppression factor of the turbulent transport coefficient is finally given as

$$\frac{\chi}{\chi_L} = \frac{1}{\left(1 - \Gamma/2 + C_1\,\Gamma^2\Gamma_c^{-2}\right)} \tag{13}$$

with

$$\Gamma_c = 2\sqrt{2}\,q\sqrt{m_e/m_i} \tag{14}$$

In the range of $\Gamma \sim \Gamma_c$, substantial reduction of the turbulent transport is expected. For the standard parameters, $q \simeq 1$ and $m_i / m_e \simeq 3600$ (i.e., Deuterium plasma), the critical asymmetry parameter Γ_c is approximately given as $\Gamma_c \simeq 0.05$. It is also noted that the critical value Γ_c is smaller for the DT-plasma compared to the D-plasmas.

The real frequency is given by Eq.(10). Noting the profile of the plasma rotation frequency, $\Delta\Omega = \hat{\Omega}\,\theta^2 / 2$, Eq.(10) indicates that the phase velocity of the mode is close to the plasma velocity at $\theta \simeq 2^{-1/4}(radian)$. Substituting the transport coefficients and the real frequency into σ, we have $\sigma_r = \left(1 + \Gamma + (2\sqrt{2} - 2)C_1\,\Gamma^2/\Gamma_c^2\right) / \sqrt{2}$ and $\sigma_i = C_2\Gamma / 2\Gamma_c$, where $C_2 = \left(\sqrt{\hat{\mu}/\hat{\chi}} + \sqrt{\hat{\chi}/\hat{\mu}}/2\right) \sim O(1)$. The eigenmode is given as

$$\tilde{p}(\eta) = exp\left\{-\frac{1}{2\sqrt{2}}\left(1 + \Gamma + (2\sqrt{2} - 2)C_1\frac{\Gamma^2}{\Gamma_c^2} + i\,\frac{C_2}{\sqrt{2}}\,\frac{\Gamma}{\Gamma_c}\right)\eta^2\right\} \tag{15}$$

Figure 1 illustrates the eigenmode structure. Owing to the inhomogeneous toroidal rotation, the mode becomes weakly propagating, and the parallel mode number is increased.

The mechanisms of turbulence suppression are explained qualitatively. The asymmetric superthermal ions have various influences on the turbulent transport induced by the ballooning mode turbulence. First, the Doppler shift modifies the dispersion relation of the ballooning mode as $\omega(\omega + k_\zeta V_\zeta) = -\gamma_{MHD}^2$, ($\gamma_{MHD}$ being the MHD growth rate).[18] Second, when the asymmetric pressure gradient exists, the effective pressure gradient is modified by the factor $(1 + \Gamma)$. Third, the parallel mode number is increased as is seen in Eq.(15). Combining these three effects, the growth rate is given as

$$\gamma^2 = (1 + \Gamma)\gamma_0^2 - k_{\parallel}^2 v_A^2 - \frac{1}{4} k_\zeta^2 V_\zeta^2 \qquad (16)$$

where $\gamma_0^2 = c_s^2/RL_p$ and L_p is the pressure gradient scale length. The asymmetric pressure gradient modifies the local pressure gradient at the bad curvature, and suppression occurs if Γ is negative. The inhomogeneous rotation on the magnetic surface increases the damping mechanisms of the second and third terms in the right hand side of Eq.(16). The latter two are independent of the sign of Γ.

This mechanism to reduce the turbulent transport is related with the "enhanced reduced shear mode". First, the nonlinear link works between the transport coefficient and electron temperature. If the electron temperature is increased and the pressure of superthermal ions builds up so as to exceed the criterion Eq.(14), then the electron thermal conductivity as well as that of ions are reduced. By this reduced transport, the electron temperature further increases. The perpendicular injection of the beam ions is effective. If the superthermal ions are localized in the high field side of the torus, Γ is negative, and the reduction of the transport is most prominent. Other key is the central localization of the heating profile. If the energetic ions are peaked, then the pressure gradient of superthermal ions is increased, giving larger Γ-parameters as is seen from Eq.(1). The peaked heating more easily causes the transport reduction of this article.

Such a situation is realized in the JT-60U experiment, where the strong central heating is made by use of the perpendicular injection from the top and bottom. The absolute value of the toroidal rotation, Ω_0, is unimportant for this mechanism. It is noted that the cooperative phenomenon appears with the reduced/negative magnetic shear. The weak-negative magnetic shear, combined with the Shafranov shift, causes the reduced transport [14]. In such a situation, the contribution of superthermal ions could be increased, and the pitch-angle scattering becomes less frequent. The anisotropic superthermal ions are more easily contained. On the other hand, the reduced transport by this new mechanism elevates the pressure gradient, and could enhance the Bootstrap current. The stronger the Bootstrap current, the larger the reduction of the magnetic shear so as to build up superthermal ions further. The reduced/negative magnetic shear is also effective from the view point of MHD stability. When the central q-value is lower than unity, the large amount of ions with large perpendicular energy could lead to the $m / n = 1 / 1$ mode instability such as the fish-bone mode.[19] If q is greater than unity, Γ could be high without causing such a deteriorating phenomenon. These relations would explain the phenomena that the internal transport barrier of electrons was unambiguously observed in the reduced-negative magnetic shear operation of the JT-60U tokamak experiments.

In summary, we here theoretically analyzed the new mechanism of the reduction of turbulent transport in high temperature tokamaks. The influence of the poloidal asymmetry of the toroidal flow, which is generated by the pressure gradient of the poloidally-asymmetric superthermal ions, is investigated. The critical level of the asymmetric pressure gradient is obtained, and this mechanism is found to be very effective in reducing the turbulent transport of the electrons.

This work is partly supported by the Grant-in-Aid for Scientific Research of Ministry of Education, Science Sports and Culture of Japan, by the collaboration program of NIFS and by the collaboration program of Advanced Fusion Center, RIAM, Kyushu University.

References

[1] F. Wagner *et al* : *Phys. Rev. Lett.* **49** 1408 (1982).

[2] S.-I. Itoh and K. Itoh: *Phys. Rev. Lett.* **60** 2276 (1988).

[3] S.-I. Itoh, K. Itoh, T. Ohkawa, N. Ueda: in *Plasma Physics and Controlled Nuclear Fusion Research 1988* (IAEA, 1989, Vienna) Vol.2, p23.

[4] K. C. Shaing *et al* : in *Plasma Physics and Controlled Nuclear Fusion Research 1988* (IAEA, 1989, Vienna) Vol.2, p13.

[5] H. Biglari, P. H. Diamond, P. W. Terry : *Phys. Fluids B* **2** 1 (1990).

[6] K. Itoh and S.-I. Itoh, *Plasma Phys. Contr. Fusion* **38** 1 (1996).

[7] M. Hugon, et al.: *Nucl. Fusion* **32** 33 (1992).

[8] Y. Koide, et al: *Phys. Rev. Lett.* **72** 366(1994).

[9] F. M. Levinton et al., *Phys. Rev. Let.* **75**, 4412 (1995).

[10] E. J. Strait et al., *Phys. Rev. Let.* **75**, 4421 (1995)

[11] K. H. Burrell, *Phys. Plasmas* **4** (1997) in press.

[12] Y. Koide, et al., *Phys. Plasmas* **4** (1997) in press.

[13] T. Ohkawa, *Research Report* NIFS-484 (1997).

[14] A. Fukuyama, et al: *Plasma Phys. Contr. Fusion* **36** 1385 (1994), A. Fukuyama, et al. *Plasma Phys. Contr. Fusion* **37** 611 (1995).

[15] S.-I. Itoh, et al, *Phys. Rev. Lett.* **72** 1200 (1994).

[16] H. Strauss, *Phys. Fluids* **20** 1354 (1977).

[17] A. Sykes et al.: in *Plasma Physics and Controlled Nuclear Fusion Research* (IAEA, 1979, Vienna) Vol.1, p.625.

[18] See, e.g., B. Lehnert, *Phys. Fluids* **9** 1367 (1966).

[19] Liu Chen, et al.: *Phys. Rev. Lett.* **52** 1122 (1984).

Figure Caption

Fig. 1 Eigenmode structure for the case of $\Gamma = \Gamma_c$. Solid line and dashed line show the real and imaginary parts, respectively. Thin and dotted line indicates the reference case with $\Gamma = 0$.

Fig.1

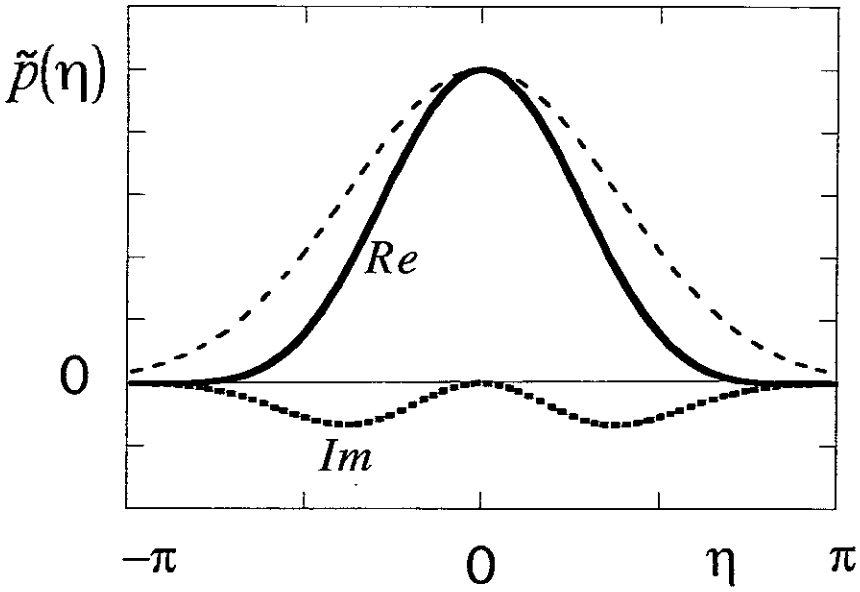

Recent Issues of NIFS Series

NIFS-450 D. Biskamp and T. Sato,
Partial Reconnection in the Sawtooth Collapse; Sep. 1996

NIFS-451 J. Li, X. Gong, L. Luo, F.X. Yin, N. Noda, B. Wan, W. Xu, X. Gao, F. Yin, J.G. Jiang, Z. Wu., J.Y. Zhao, M. Wu, S. Liu and Y. Han,
Effects of High Z Probe on Plasma Behavior in HT-6M Tokamak; Sep. 1996

NIFS-452 N. Nakajima, K. Ichiguchi, M. Okamoto and R.L. Dewar,
Ballooning Modes in Heliotrons/Torsatrons; Sep. 1996 (IAEA-CN-64/D3-6)

NIFS-453 A. Iiyoshi,
Overview of Helical Systems; Sep. 1996 (IAEA-CN-64/O1-7)

NIFS-454 S. Saito, Y. Nomura, K. Hirose and Y.H. Ichikawa,
Separatrix Reconnection and Periodic Orbit Annihilation in the Harper Map; Oct. 1996

NIFS-455 K. Ichiguchi, N. Nakajima and M. Okamoto,
Topics on MHD Equilibrium and Stability in Heliotron / Torsatron; Oct. 1996

NIFS-456 G. Kawahara, S. Kida, M. Tanaka and S. Yanase,
Wrap, Tilt and Stretch of Vorticity Lines around a Strong Straight Vortex Tube in a Simple Shear Flow; Oct. 1996

NIFS-457 K. Itoh, S.- I. Itoh, A. Fukuyama and M. Yagi,
Turbulent Transport and Structural Transition in Confined Plasmas; Oct. 1996

NIFS-458 A. Kageyama and T. Sato,
Generation Mechanism of a Dipole Field by a Magnetohydrodynamic Dynamo; Oct. 1996

NIFS-459 K. Araki, J. Mizushima and S. Yanase,
The Non-axisymmetric Instability of the Wide-Gap Spherical Couette Flow; Oct. 1996

NIFS-460 Y. Hamada, A. Fujisawa, H. Iguchi, A. Nishizawa and Y. Kawasumi,
A Tandem Parallel Plate Analyzer; Nov. 1996

NIFS-461 Y. Hamada, A. Nishizawa, Y. Kawasumi, A. Fujisawa, K. Narihara, K. Ida, A. Ejiri, S. Ohdachi, K. Kawahata, K. Toi, K. Sato, T. Seki, H. Iguchi, K. Adachi, S. Hidekuma, S.Hirokura, K. Iwasaki, T. Ido, M. Kojima, J. Koong, R. Kumazawa, H. Kuramoto, T. Minami, I. Nomura, H. Sakakita, M. Sasao, K.N. Sato, T. Tsuzuki, J. Xu, I. Yamada and T. Watari,
Density Fluctuation in JIPP T-IIU Tokamak Plasmas Measured by a Heavy Ion Beam Probe; Nov. 1996

NIFS-462 N. Katsuragawa, H. Hojo and A. Mase,
Simulation Study on Cross Polarization Scattering of Ultrashort-Pulse Electromagnetic Waves; Nov. 1996

NIFS-463 V. Voitsenya, V. Konovalov, O. Motojima, K. Narihara, M. Becker and B. Schunke,
Evaluations of Different Metals for Manufacturing Mirrors of Thomson Scattering System for the LHD Divertor Plasma; Nov. 1996

NIFS-464 M. Pereyaslavets, M. Sato, T. Shimozuma, Y. Takita, H. Idei, S. Kubo, K. Ohkubo and K. Hayashi,
Development and Simulation of RF Components for High Power Millimeter Wave Gyrotrons; Nov. 1996

NIFS-465 V.S. Voitsenya, S. Masuzaki, O. Motojima, N. Noda and N. Ohyabu,
On the Use of CX Atom Analyzer for Study Characteristics of Ion Component in a LHD Divertor Plasma; Dec. 1996

NIFS-466 H. Miura and S. Kida,
Identification of Tubular Vortices in Complex Flows; Dec. 1996

NIFS-467 Y. Takeiri, Y. Oka, M. Osakabe, K. Tsumori, O. Kaneko, T. Takanashi, E. Asano, T. Kawamoto, R. Akiyama and T. Kuroda,
Suppression of Accelerated Electrons in a High-current Large Negative Ion Source; Dec. 1996

NIFS-468 A. Sagara, Y. Hasegawa, K. Tsuzuki, N. Inoue, H. Suzuki, T. Morisaki, N. Noda, O. Motojima, S. Okamura, K. Matsuoka, R. Akiyama, K. Ida, H. Idei, K. Iwasaki, S. Kubo, T. Minami, S. Morita, K. Narihara, T. Ozaki, K. Sato, C. Takahashi, K. Tanaka, K. Toi and I. Yamada,
Real Time Boronization Experiments in CHS and Scaling for LHD; Dec. 1996

NIFS-469 V.L. Vdovin, T.Watari and A. Fukuyama,
3D Maxwell-Vlasov Boundary Value Problem Solution in Stellarator Geometry in Ion Cyclotron Frequency Range (final report); Dec. 1996

NIFS-470 N. Nakajima, M. Yokoyama, M. Okamoto and J. Nührenberg,
Optimization of M=2 Stellarator; Dec. 1996

NIFS-471 A. Fujisawa, H. Iguchi, S. Lee and Y. Hamada,
Effects of Horizontal Injection Angle Displacements on Energy Measurements with Parallel Plate Energy Analyzer; Dec. 1996

NIFS-472 R. Kanno, N. Nakajima, H. Sugama, M. Okamoto and Y. Ogawa,
Effects of Finite-β and Radial Electric Fields on Neoclassical Transport in the Large Helical Device; Jan. 1997

NIFS-473 S. Murakami, N. Nakajima, U. Gasparino and M. Okamoto,
Simulation Study of Radial Electric Field in CHS and LHD; Jan. 1997

NIFS-474 K. Ohkubo, S. Kubo, H. Idei, M. Sato, T. Shimozuma and Y. Takita,
Coupling of Tilting Gaussian Beam with Hybrid Mode in the Corrugated Waveguide; Jan. 1997

NIFS-475 A. Fujisawa, H. Iguchi, S. Lee and Y. Hamada,
Consideration of Fluctuation in Secondary Beam Intensity of Heavy Ion Beam Prove Measurements; Jan. 1997

NIFS-476 Y. Takeiri, M. Osakabe, Y. Oka, K. Tsumori, O. Kaneko, T. Takanashi, E. Asano, T. Kawamoto, R. Akiyama and T. Kuroda,
Long-pulse Operation of a Cesium-Seeded High-Current Large Negative Ion Source; Jan. 1997

NIFS-477 H. Kuramoto, K. Toi, N. Haraki, K. Sato, J. Xu, A. Ejiri, K. Narihara, T. Seki, S. Ohdachi, K. Adati, R. Akiyama, Y. Hamada, S. Hirokura, K. Kawahata and M. Kojima,
Study of Toroidal Current Penetration during Current Ramp in JIPP T-IIU with Fast Response Zeeman Polarimeter; Jan., 1997

NIFS-478 H. Sugama and W. Horton,
Neoclassical Electron and Ion Transport in Toroidally Rotating Plasmas; Jan. 1997

NIFS-479 V.L. Vdovin and I.V. Kamenskij,
3D Electromagnetic Theory of ICRF Multi Port Multi Loop Antenna; Jan. 1997

NIFS-480 W.X. Wang, M. Okamoto, N. Nakajima, S Murakami and N. Ohyabu,
Cooling Effect of Secondary Electrons in the High Temperature Divertor Operation; Feb. 1997

NIFS-481 K. Itoh, S.-I. Itoh, H. Soltwisch and H.R. Koslowski,
Generation of Toroidal Current Sheet at Sawtooth Crash; Feb. 1997

NIFS-482 K. Ichiguchi,
Collisionality Dependence of Mercier Stability in LHD Equilibria with Bootstrap Currents; Feb. 1997

NIFS-483 S. Fujiwara and T. Sato,
Molecular Dynamics Simulations of Structural Formation of a Single Polymer Chain: Bond-orientational Order and Conformational Defects; Feb. 1997

NIFS-484 T. Ohkawa,
Reduction of Turbulence by Sheared Toroidal Flow on a Flux Surface; Feb. 1997

NIFS-485 K. Narihara, K. Toi, Y. Hamada, K. Yamauchi, K. Adachi, I. Yamada, K. N. Sato, K. Kawahata, A. Nishizawa, S. Ohdachi, K. Sato, T. Seki, T. Watari, J. Xu, A. Ejiri, S. Hirokura, K. Ida, Y. Kawasumi, M. Kojima, H. Sakakita, T. Ido, K. Kitachi, J. Koog and

H. Kuramoto,
Observation of Dusts by Laser Scattering Method in theJIPPT-IIU Tokamak
Mar. 1997

NIFS-486 S. Bazdenkov, T. Sato and The Complexity Simulation Group,
Topological Transformations in Isolated Straight Magnetic Flux Tube; Mar. 1997

NIFS-487 M. Okamoto,
Configuration Studies of LHD Plasmas; Mar. 1997

NIFS-488 A. Fujisawa, H. Iguchi, H. Sanuki, K. Itoh, S. Lee, Y. Hamada, S. Kubo, H. Idei, R. Akiyama, K. Tanaka, T. Minami, K. Ida, S. Nishimura, S. Morita, M. Kojima, S. Hidekuma, S.-I. Itoh, C. Takahashi, N. Inoue, H. Suzuki, S. Okamura and K. Matsuoka,
Dynamic Behavior of Potential in the Plasma Core of the CHS Heliotron/Torsatron; Apr. 1997

NIFS-489 T. Ohkawa,
Pfirsch - Schlüter Diffusion with Anisotropic and Nonuniform Superthermal Ion Pressure; Apr. 1997

NIFS-490 S. Ishiguro and The Complexity Simulation Group,
Formation of Wave-front Pattern Accompanied by Current-driven Electrostatic Ion-cyclotron Instabilities; Apr. 1997

NIFS-491 A. Ejiri, K. Shinohara and K. Kawahata,
An Algorithm to Remove Fringe Jumps and its Application to Microwave Reflectometry; Apr. 1997

NIFS-492 K. Ichiguchi, N. Nakajima, M. Okamoto,
Bootstrap Current in the Large Helical Device with Unbalanced Helical Coil Currents; Apr. 1997

NIFS-493 S. Ishiguro, T. Sato, H. Takamaru and The Complexity Simulation Group,
V-shaped dc Potential Structure Caused by Current-driven Electrostatic Ion-cyclotron Instability; May 1997

NIFS-494 K. Nishimura, R. Horiuchi, T. Sato,
Tilt Stabilization by Energetic Ions Crossing Magnetic Separatrix in Field-Reversed Configuration; June 1997

NIFS-495 T. -H. Watanabe and T. Sato,
Magnetohydrodynamic Approach to the Feedback Instability; July 1997

NIFS-496 K. Itoh, T. Ohkawa, S. -I. Itoh, M. Yagi and A. Fukuyama
Suppression of Plasma Turbulence by Asymmetric Superthermal Ions; July 1997